

RESEARCH PAPER

The form of nitrogen nutrition affects resistance against *Pseudomonas syringae* pv. *phaseolicola* in tobacco

Kapuganti J. Gupta^{1,*†}, Yariv Brotman², Shruthi Segu², Tatiana Zeier³, Jürgen Zeier³, Stefan T. Persijn⁴, Simona M. Cristescu⁵, Frans J. M. Harren⁵, Hermann Bauwe¹, Alisdair R. Fernie², Werner M. Kaiser⁶ and Luis A. J. Mur^{7,†}

¹ Department of Plant Physiology, University of Rostock, Albert Einstein Str 3, D-18059, Rostock, Germany

² Max-Planck-Institute of Molecular Plant Physiology, Am Mühlenberg 1, D-14476 Golm-Potsdam, Germany

³ Institute for Plant Molecular Ecophysiology, Heinrich-Heine-Universität Universitätsstrasse 1 40225 Düsseldorf

⁴ Dutch Metrology Institute, VSL, Thijssseweg 11, 2629 JA Delft, The Netherlands

⁵ Molecular and Laser Physics, Radboud University Nijmegen, 6500 GL Nijmegen, The Netherlands

⁶ Lehrstuhl Botanik I, Julius-von-Sachs-Institut für Biowissenschaften, Universität Würzburg, Julius-von-Sachs-Platz 2, D-97082 Würzburg, Germany

⁷ Aberystwyth University, Institute of Environmental and Rural Science, Edward Llwyd Building, Aberystwyth, UK, SY23 3DA

* Present address: Department of Plant Sciences, University of Oxford, South Parks Road, Oxford OX1 3RB, UK.

† To whom correspondence should be addressed. E-mail: jagadis.kapuganti@plants.ox.ac.uk or lum@aber.ac.uk

Received 3 August 2012; Revised 5 November 2012; Accepted 8 November 2012

Abstract

Different forms of nitrogen (N) fertilizer affect disease development; however, this study investigated the effects of N forms on the hypersensitivity response (HR)—a pathogen-elicited cell death linked to resistance. HR-eliciting *Pseudomonas syringae* pv. *phaseolicola* was infiltrated into leaves of tobacco fed with either NO_3^- or NH_4^+ . The speed of cell death was faster in NO_3^- -fed compared with NH_4^+ -fed plants, which correlated, respectively, with increased and decreased resistance. Nitric oxide (NO) can be generated by nitrate reductase (NR) to influence the formation of the HR. NO generation was reduced in NH_4^+ -fed plants where N assimilation bypassed the NR step. This was similar to that elicited by the disease-forming *P. syringae* pv. *tabaci* strain, further suggesting that resistance was compromised with NH_4^+ feeding. *PR1a* is a biomarker for the defence signal salicylic acid (SA), and expression was reduced in NH_4^+ -fed compared with NO_3^- fed plants at 24 h after inoculation. This pattern correlated with actual SA measurements. Conversely, total amino acid, cytosolic and apoplastic glucose/fructose and sucrose were elevated in NH_4^+ -treated plants. Gas chromatography/mass spectroscopy was used to characterize metabolic events following different N treatments. Following NO_3^- nutrition, polyamine biosynthesis was predominant, whilst after NH_4^+ nutrition, flux appeared to be shifted towards the production of 4-aminobutyric acid. The mechanisms whereby NO_3^- feeding enhances SA, NO, and polyamine-mediated HR-linked defence whilst these are compromised with NH_4^+ , which also increases the availability of nutrients to pathogens, are discussed.

Key words: ammonium, hypersensitive response, nitrate, nitric oxide, *Pseudomonas*, tobacco.

Abbreviations: GABA, 4-aminobutyric acid; GC-MS, gas chromatography/mass spectroscopy; GS, glutamine synthetase; HR, hypersensitivity response; N, nitrogen; NO, nitric oxide; NR, nitrate reductase; PPDF, photosynthetic photon flux density; Psph, *Pseudomonas syringae* pv. *phaseolicola*; Pt, *P. syringae* pv. *tabaci*; QCL, quantum cascade laser; qRT-PCR, quantitative real-time RT-PCR; SA, salicylic acid; TCA, tricarboxylic acid.

© 2012 The Authors.

This is an Open Access article distributed under the terms of the Creative Commons Attribution Non-Commercial License (<http://creativecommons.org/licenses/by-nc/2.0/uk/>) which permits unrestricted non-commercial use, distribution, and reproduction in any medium, provided the original work is properly cited.

Introduction

The anthropogenic application of nitrogen (N) fertilizer has been a major factor in modern high crop yields and plant quality (Tilman, 1999; Hajjar and Hodgkin, 2007). This has resulted in a doubling of N loads to soil since the beginning of the 20th century (Green *et al.*, 2004) and is continuing with total global N inputs in the region of 150 teragrams of N year⁻¹ (Schlesinger, 2009). In agricultural soils, N is supplied in the form of nitrate (NO₃⁻), ammonium (NH₄⁺), or a combination of both. Plants will reduce NO₃⁻ using nitrate reductase (NR) to generate NO₂⁻, which is further reduced to NH₄⁺, which can be directly assimilated by glutamine synthetase (GS) to form glutamine. NH₄⁺ can also enter the soil biosystem via fixation of atmospheric N, as well as by decomposition of organic matter by microorganisms such as bacteria and fungi. NH₄⁺ can be oxidized to first NO₂⁻ and subsequently to NO₃⁻ by the nitrification pathway. Given its widespread use, the agricultural impact of N nutrition on disease development has been extensively examined (Huber and Watson, 1974). However, here we have assessed the effects of the form of N nutrition on a form of resistance to pathogens that is typified by the hypersensitivity response (HR).

When a pathogen first comes into contact with a host, it is assumed to be nutrient starved, meaning that rapid assimilation of host nutrients is essential for successful pathogenesis (Snoeijs *et al.*, 2000). Equally, the host seeks to either prevent this and/or mobilize its nutrients to further defence responses. These opposing aims are well exemplified in the changes in N metabolism seen during plant–pathogen interactions. The accumulation of 4-aminobutyric acid (GABA)—a glutamate-derived metabolite—has been observed in response to a range of biotic stresses (Kinnersley and Turano, 2000). In the case of infection of tomato by *Cladosporium fulvum*, GABA has been shown to be utilized by the pathogen (Kinnersley and Turano, 2000; Solomon and Oliver, 2001), but from the perspective of the host, GABA participates in the so-called ‘GABA shunt’, allowing a direct link between reduced N in the host (as represented in GABA) and the tricarboxylic acid (TCA) cycle (Fromm and Bouche, 2004). This may occur due to the host’s increased bioenergetic requirements following infection (Fait *et al.*, 2008). Some N manipulation can be more obviously favourable to the pathogen. For example, several genes usually associated with N mobilization during senescence, such as specific forms of GS, as well as some senescence-associated genes, are induced during disease (Bender *et al.*, 1999; Pontier *et al.*, 1999; Quirino *et al.*, 1999; Masclaux *et al.*, 2000). Similarly, infection of French bean (*Phaseolus vulgaris*) by the anthracnose pathogen *Colletotrichum lindemuthianum* induces GS expression (Tavernier *et al.*, 2007). Furthermore, as C:N assimilatory links are well established (Fritz *et al.*, 2006a; Bauwe *et al.*, 2010; Sweetlove *et al.*, 2010), it is unsurprising that N changes correlate with increase host-cell sugar export to influence plant disease susceptibility (Tadege *et al.*, 1998; Thibaud *et al.*, 2004). Thus, whilst N fertilizers improve the nutrient status of the host, they can also promote disease (Huber and Watson, 1974).

Co-application of biocides with N fertilizers may appear to be a worthwhile agricultural strategy to negate any disease-promoting effects of the latter. However, there is increasing pressure to reduce the use of a range of biocides in agriculture (Gullino and Kuijpers, 1994) and to exploit endogenous plant defence mechanisms in plant breeding and agricultural practice. The introgression of resistance (R) genes into elite crop germplasm has been, and remains, an important approach to securing yields (Rommens and Kishore, 2000). One consequence of R gene-mediated resistance is often the elicitation of a programmed cell death—the hypersensitivity response (HR). N effects appear to be a facet of HR-mediated resistance, as elicitation of the HR induces GS and glutamate dehydrogenase via the defence hormone salicylic acid (SA) and could aid in mobilizing N away from the pathogen (Pageau *et al.*, 2006). Another N component in plant defence is nitric oxide (NO), which is a major contributor to the formation of the HR (Delledonne *et al.*, 1998; Gupta, 2011). Crucially, under aerobic conditions, NO is generated by NR acting on the reduced product of a NADPH-dependent nitrite reductase (Molodo *et al.*, 2005; Gupta *et al.*, 2011). As NR cannot act on NH₄⁺, the type of N nutrition (NO₃⁻ or NH₄⁺) would influence whether NO were generated. NO initiates the biosynthesis of SA via a signalling route that involves cyclic GMP and cyclic ADP-ribose (Durner and Klessig, 1999). SA is an important stress signal, and is known to play important roles in HR-type plant defence (Mur *et al.*, 2000, 2008), thermotolerance (Clarke *et al.*, 2004), chilling (Scott *et al.*, 2004), and stomatal regulation (Khokon *et al.*, 2011). The physiological link between NO and SA effects have been shown in localized plant defence (Klessig *et al.*, 2000), systemic acquired resistance (Espunya *et al.*, 2012), and stomatal opening (Sun *et al.*, 2010).

Here, we characterized the influence of NO₃⁻ or NH₄⁺ nutrition on HR-mediated resistance, focusing on the impact on NO, SA, and primary plant metabolism. We have shown how NO₃ feeding augments HR-mediated resistance, whilst NH₄ can compromise defence by mechanisms, which include increasing nutrient availability for the pathogen.

Materials and methods

Plant materials

Tobacco seeds cv. Gatersleben were germinated on vermiculite in a day/night regime of 14/10 h, 24/20 °C, a relative humidity of 80%, and photosynthetic photon flux density (PPFD) of 350–400 μmol m⁻² s⁻¹. After 3 weeks, the plants were transferred to hydroponic culture for an additional 4–8 weeks. Plastic pots, each containing 1.8 l of nutrient solution, were kept in a growth chamber with artificial illumination (HQI 400 W; Schreder, Winterbach, Germany) at PPFD of 300 μmol m⁻² s⁻¹ and with 16 h daily light periods. The day/night temperature regime of the chamber was 24/20 °C. Nutrient solution was prepared according to the method of Planchet *et al.* (2005). The NO₃⁻ nutrient solution (pH 6.3) contained 3 mM KNO₃, 1 mM CaCl₂, 1 mM MgSO₄, 25 μM NaFe-EDTA, 0.5 mM K₂HPO₄, 1 mM KH₂PO₄, and trace elements according to Planchet *et al.* (2005). For NH₄⁺-fed plants, the nutrient solution was: 3 mM NH₄Cl,

1 mM CaCl₂, 1 mM MgSO₄, 25 μM NaFe-EDTA, 0.5 mM K₂HPO₄, 1 mM KH₂PO₄, and trace elements. The composition of the nutrient solution for the NR-deficient *Nia30* Gatersleben mutant was: 1 mM KNO₃, 3 mM NH₄Cl initially for 1 week and 3 mM NH₄Cl thereafter, 1 mM CaCl₂, 1 mM MgSO₄, 25 μM NaFe-EDTA, 2 mM KH₂PO₄/K₂HPO₄, and trace elements. For all these conditions, nutrient solutions were changed three times a week. Some tobacco plants were also grown in low-nutrient John Innes Seed Compost (William Sinclair Horticulture, UK) and watered with NO₃⁻ or NH₄⁺ nutrient solutions (as detailed above) every 2 d as appropriate to the experiment. In experiments where compost-grown plants were used, this is indicated in the text.

Growth of plant pathogens, plant inoculation, and estimation of in planta bacterial populations

Pseudomonas syringae pv. *phaseolicola* strain 1448A (*PspH*) and *P. syringae* pv. *tabaci* strain 4152 (*Pt*) (both rifampicin resistant) were grown at 28 °C in King's B medium containing rifampicin (10 mg ml⁻¹) (Zeier *et al.*, 2004). Overnight exponential-phase cultures were washed three times with autoclaved 10 mM MgCl₂ and diluted to a final concentration of 10⁵ cells ml⁻¹. The bacterial suspensions were infiltrated from the abaxial side into a sample leaf using a 1 ml syringe with a needle. Control inoculations were performed with 10 mM MgCl₂. *In planta* bacterial population sizes were assessed to indicate the extent of resistance/susceptibility exhibited by the host. Cores of 1 cm discs (0.79 cm²) were taken using a cork borer and ground down in a mortar and pestle and resuspended in 1 ml of 10 mM MgCl₂. Serial dilutions of the slurry were plated on rifampicin (10 mg ml⁻¹)-supplemented King's B medium and incubated at 30 °C until colonies formed. Based on the number of colonies and dilution factor, the original *in planta* population was calculated.

Estimations of electrolyte leakage

Loss of membrane integrity was estimated by electrolyte leakage in 1 cm diameter cores as described by Mur *et al.* (1997). This measure was used to suggest the kinetics of cell death.

NO measurement

Quantum cascade laser (QCL) The use of a QCL to detect NO has been described recently (Mur *et al.*, 2011). The system allows real-time NO measurements with a detection limit of 0.8 ppbv s⁻¹ (Cristescu *et al.*, 2008). Before each experiment, the QCL was calibrated against gas mixtures prepared from a reference gas mixture (100 ppbv NO in N₂) diluted in NO-free air to cover the range 10–100 ppbv. Infiltrated tobacco leaves that had been detached at the petiole were placed in a 200 ml glass cuvette in an inlet and outlet carrier flow of air via gas tubing, and NO production was monitored at a controlled continuous flow rate of 1 l h⁻¹. During NO measurements, the leaves in the cuvette were maintained in a Sanyo MLR-350 environmental test chamber at 20 °C under a 16 h light (200 μmol m⁻² s⁻¹)/ 8 h dark regime. The humidity within the cuvette was not controlled or measured.

Multiple cuvettes could be monitored in sequence, each being measured for ~13 min. The laser light emitted by the QCL around 1850 cm⁻¹ passed through a multi-pass absorption cell where the NO molecules were transported via the gastube. The intensity of the transmitted laser light was attenuated due to the NO absorption of the light in the multi-pass cell (effective path length=76 m), following the Beer–Lambert law. The detected signal depended on the laser intensity before the multi-pass cell, the absorption length, and the absorption coefficient of NO at the particular wavelength. The NO concentration was calculated by measuring attenuation of the light coming into the cell relative to the transmitted light (after the cell).

Chemiluminescence

For experiments with detached leaves, the leaves were cut off from the plant and placed in nutrient solution, where the petiole was cut off a second time below the solution surface. The leaves (petiole in nutrient solution) were placed in a transparent lid chamber with 2 or 4 l of air volume, depending on leaf size and number. A constant flow of measuring gas (purified air or N₂) at 1.5 l min⁻¹ was pulled through the chamber and subsequently through the chemiluminescence detector (CLD 770 AL ppt; Eco-Physics, Dürnten, Switzerland; detection limit 20 ppt; 10 s time resolution) by a vacuum pump connected to an ozone destroyer. The ozone generator of the chemiluminescence detector was supplied with dry oxygen (99%). The measuring gas (air or N₂) was made NO free by conducting it through a custom-made charcoal column (1 m long, 3 cm internal diameter, particle size 2 mm). Calibration was carried out routinely with NO-free air (0 ppt NO) and with various concentrations of NO (1–35 ppb) adjusted by mixing the calibration gas (500 ppb NO in N₂; Messer Griesheim, Darmstadt, Germany) with NO-free air. Flow controllers (FC-260; Tylan General, Eching, Germany) were used to adjust all gas flows. Light was provided by a 400 W HQI lamp (Schreder) above the cuvette. Quantum flux density could be adjusted within limits (150–400 μmol m⁻² s⁻¹ PPDF) by changing the distance between the lamp and cuvette. The air temperature in the cuvette was monitored continuously and was usually about 20 °C in the dark and 23–25 °C in the light.

Expression profiling by quantitative real-time RT-PCR (qRT-PCR)

Expression analysis was performed using an expression profiling platform of the response of eight defence genes against *Pseudomonas* in tobacco. Primer sequences were designed using QuantPrime (Arvidsson *et al.*, 2008). Fully expanded leaves were collected and pooled from six plants in each treatment. Total RNA was purified using an RNeasy Mini Kit (Qiagen, <http://www.qiagen.com>) and DNase digestion was performed with a Turbo DNA-free Kit (Ambion, <http://www.ambion.com/>). Four micrograms of total RNA was used as template for first-strand cDNA synthesis with a RevertAid cDNA Synthesis Kit (Fermentas, <http://www.fermentas.com/>). cDNA (20 ng) was used for qRT-PCR with Power SYBR Green reagent performed on an ABI PRISM 7900HT sequence detection system (Applied Biosystems, <http://www.appliedbiosystems.com/>). Data were analysed with the 7900 version 2.0.3 evaluation software (Applied Biosystems). The fold change in the target genes was normalized to a reference gene, elongation factor 1a (*EF1a*). Fold expression relative to control plants was determined using the ΔΔC_T method, as described by Libault *et al.* (2007). Three biological experiments (with two independent replicates for each experiment) were performed for each treatment. Comparisons of gene expression between the different treatments compared with the control were conducted using a *t*-test.

Extraction of apoplastic fluid

Apoplastic fluid was extracted from tobacco leaves by direct centrifugation as described by Dannel *et al.* (1995), with some modifications. Leaves were cut at the base of the petiole with a sharp razor blade and the petiole immediately immersed in

deionized water. Each leaf was then rolled into several folds and placed into a plastic syringe (25 ml) with the petiole side at the base of the syringe. The syringe was placed in a 50 ml centrifuge tube. Leaf-filled syringes were centrifuged at 4 °C at 4000g and apoplastic fluid was collected from the bottom of the centrifuge tube.

Targeted sugar and total amino acid measurements

Major sugars (glucose, fructose, and sucrose) were separated by anion-exchange chromatography (0.1 N NaOH as the eluent) on a Carboxypac column plus pre-column and detected directly by pulsed amperometry (Dionex 4500i; Dionex, Idstein, Germany). Total amino acids were measured by HPLC, as described by Mahmood *et al.* (2002).

Metabolite profiling

Gas chromatography/mass spectroscopy (GC-MS) analysis was performed as described previously (Lisec *et al.*, 2006). Six replicates each consisting of six pooled plants obtained from two independent experiments were subjected to GC-MS analysis. Metabolite levels were determined in a targeted fashion using the TargetSearch software package (Cuadros-Inostroza *et al.*, 2009). Metabolites were selected by comparing their retention indexes (± 2 s) and spectra (similarity >85%) against compounds stored in the Golm Metabolome Database (Kopka *et al.*, 2005). This resulted in 150 metabolites, which were kept in the data matrix. Each metabolite was represented by the observed ion intensity of a selected unique ion, which allowed relative quantification between groups. Metabolite data were \log_{10} -transformed to improve normality (Steinfath *et al.*, 2008) and normalized to show identical medium peak sizes per sample group.

Data analyses

Metabolite data were analysed by multivariate approaches using Pychem software (Jarvis *et al.*, 2006). Where the statistical test for significant was between two groups, *t*-tests were used, but when comparing between three or more groups Tukey's multiple pairwise comparison test was employed using Minitab version 14 (Minitab, Coventry, UK). The Tukey test outputs represent adjusted *P* values based on significant differences between differing datasets. Datasets where there were no significant differences are indicated on the figures using alphabetical indicators.

Results

The form of N nutrition influences HR development induced by *Psph*

To investigate the role of NO_3^- and NH_4^+ nutrition on HR-associated defence, tobacco cv. Gatersleben plants were grown in hydroponic solutions containing either 3 mM KNO_3 (referred to as NO_3^- -fed plants) or 3 mM NH_4Cl (referred to as NH_4^+ -fed plants) for 1 week and then challenged with

Psph. Within 24h post-inoculation (p.i.), leaf discoloration was observed at the inoculation sites of NO_3^- -treated plants only (Fig. 1A). To quantify the loss of membrane integrity, which is linked to cell death, electrolyte leakage from isolated explants of *Psph*-challenged tissue was assessed (Fig. 1B). Leakage was more rapid in NO_3^- -fed compared with NH_4^+ -fed plants, which tallied with the observed differences in macrolesion formation (Fig. 1A). To link these changes with host resistance *in planta*, *Psph* population sizes were determined (Fig. 1C). No significant differences in bacterial numbers within NO_3^- -fed compared with NH_4^+ -fed plants were observed, and in both, growth from the initial population (0 d p.i.) was evident. However, at 7 days p.i., whereas in NH_4^+ -fed plants there was a significant ($P < 0.001$) increase in bacterial numbers compared with 3 days p.i., with NO_3^- -fed plants the bacterial numbers were reduced. This delay in the HR observed for NH_4^+ -treated plants was linked with increased *Psph* growth *in planta* (Fig. 1C), suggesting that resistance was compromised. However, with NO_3^- -fed plants, there was a dramatic reduction in bacterial numbers at 7 days p.i., which seemed to be associated with a more rapid cell death (Fig. 1B). To investigate further whether HR-linked resistance was comprised in *Psph* in NH_4^+ -fed tobacco, comparisons were made with electrolyte leakage and bacterial populations in leaves inoculated with the virulent bacterial pathogen *Pt* in tobacco plants fed with either NH_4^+ or NO_3^- (Fig. 1B and C). The rate of electrolyte leakage in explants from *Pt*-inoculated leaves was slower than that seen in explants from *Psph*-challenged NH_4^+ -fed or NO_3^- -fed plants. Similarly, *Pt* populations were more abundant than *Psph* in any tobacco plants. Taken together, these results indicated that HR resistance to *Psph* was reduced but not abolished in NH_4^+ -fed tobacco. Interestingly, *Pt* populations in NO_3^- -fed tobacco were significantly ($P < 0.001$) reduced compared with NH_4^+ -fed plants but were significantly ($P < 0.001$) greater than any measured for *Psph* (Fig. 1C).

It has been demonstrated that NO is involved in the cell death process during the HR (Delledonne *et al.*, 1998), and NO_3^- nutrition is known to influence NO levels (Planchet *et al.*, 2005). Thus, we tested whether N nutrition had an impact on NO generation in the course of an HR elicited by *Psph* in tobacco. Initially, we used low-nutrient compost-grown tobacco plants, which were supplemented with either NH_4^+ or NO_3^- feed. NO production was measured from *Psph*-infected tobacco plants using a QCL (Mur *et al.*, 2011). We observed that NO production was greater in NO_3^- -fed and *Psph*-challenged plants compared with their NH_4^+ -fed equivalents (Fig. 2A). No NO production could be detected from uninfected plants (data not shown). We partially corroborated these observations by a second independent determination of NO levels in hydroponically grown plants using the gas-phase chemiluminescence method. This indicated greater NO emission from NO_3^- -grown and *Psph* challenged leaves compared with NH_4^+ -fed plants (Fig. 2B). The difference in quantitative values for NO emissions measured by chemiluminescence compared with QCL is likely to reflect a difference between *Psph*-challenged, soil-grown and hydroponically grown tobacco plants, respectively.

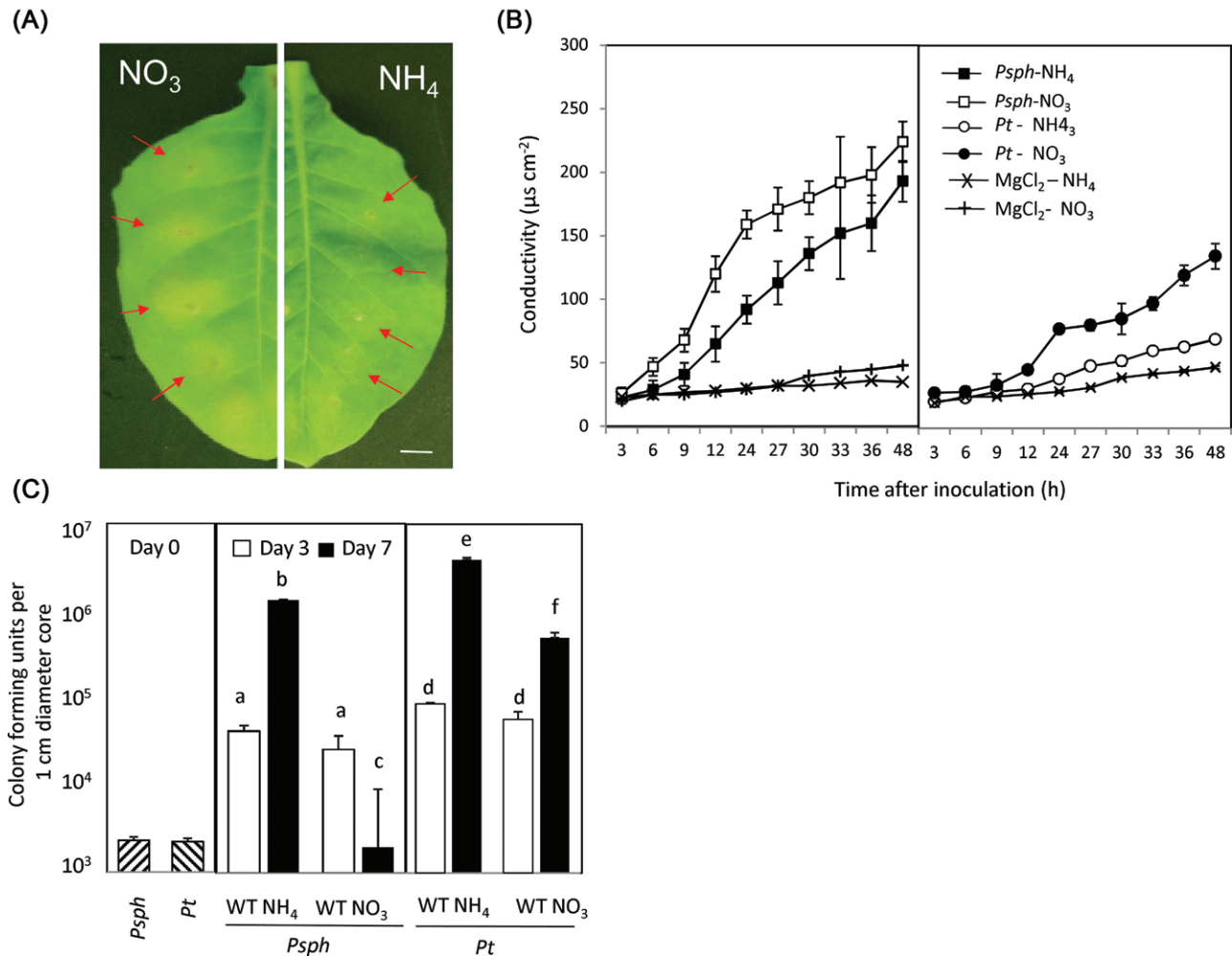


Fig. 1. Forms of N fertilizer influence the HR elicited by *Psph* in tobacco. (A) Lesion development (arrows) at 24 h p.i. of NO_3^- -fed or NH_4^+ -fed tobacco leaves with avirulent *Psph*. Plants were grown hydroponically as described in Materials and methods, and 1 week prior to inoculation, the plants were transferred to NO_3^- (5 mM) or NH_4^+ (5 mM) growth medium. Half leaves are shown and illustrate how the responses were more advanced in NO_3^- -fed compared with NH_4^+ -fed leaves. The results are representative of three independent experiments. Bar, 1 cm. (B) Electrolyte leakage from 1 cm diameter leaf discs sampled from areas of NO_3^- -fed or NH_4^+ -fed plants and inoculated with *Psph*, *Pt*, or 10 mM MgCl_2 (control). Electrolyte leakage from the 10 mM MgCl_2 infiltrated discs shows the baseline changes occurring from simple coring of leaf tissue. (C) *Psph* and *Pt* populations in NO_3^- -fed or NH_4^+ -fed tobacco plants at 3 and 7 d with *Psph* [$n=6$; results shown as means \pm standard deviation (SD)]. The initial populations of *Psph* and *Pt* as assessed immediately after infiltration (at 0 d) are also shown. Different letters denote groupings within which non-significant differences were observed but which were significantly different ($P < 0.05$) from all other groups.

Rates of NO production from *Pt*-inoculated NH_4^+ -fed and NO_3^- -fed tobacco were also measured in compost-grown plants using QCL (Fig. 2A). NO production in NH_4^+ -fed, *Pt*-inoculated plants did not differ significantly from those seen with NH_4^+ -fed, *Psph*-challenged plants. Thus, it was not possible to correlate exactly *in planta* the bacterial populations in *Pt*-infected plants and *Psph*-challenged NH_4^+ -fed plants (Fig. 1C) with NO production. However, more NO was observed with *Pt*-infected NO_3^- -fed plants compared with NH_4^+ -fed plants, which could explain the decreased bacterial populations seen in the latter (Fig. 1C).

To substantiate the link between NO production and cell death and a loss in bacterial resistance, we examined the interaction of *Psph* with the tobacco NR- mutant *Nia30* line

(supplied with NO_3^- plus NH_4^+) (Supplementary Fig. S1 at JXB online). Using the QCL method, NO production was shown to be suppressed in *Nia30* plants, and indeed more than in inoculated NH_4^+ -treated wild-type plants (Supplementary Fig. S1A). This correlated with a reduction in *Psph*-associated electrolyte leakage in *Nia30* plants (Supplementary Fig. S1B) and increased bacterial numbers in *Nia30* plants compared with NH_4^+ -fed wild-type tobacco (Supplementary Fig. S1C). These data could indicate that NR is a major source of NO during *Psph* infection but that NH_4 feeding could only partially mimic this situation. However, equally, the data could reflect that these plants were grown in low-nutrient compost rather than hydroponic conditions so some NO_3 could have been supplied to the plant.

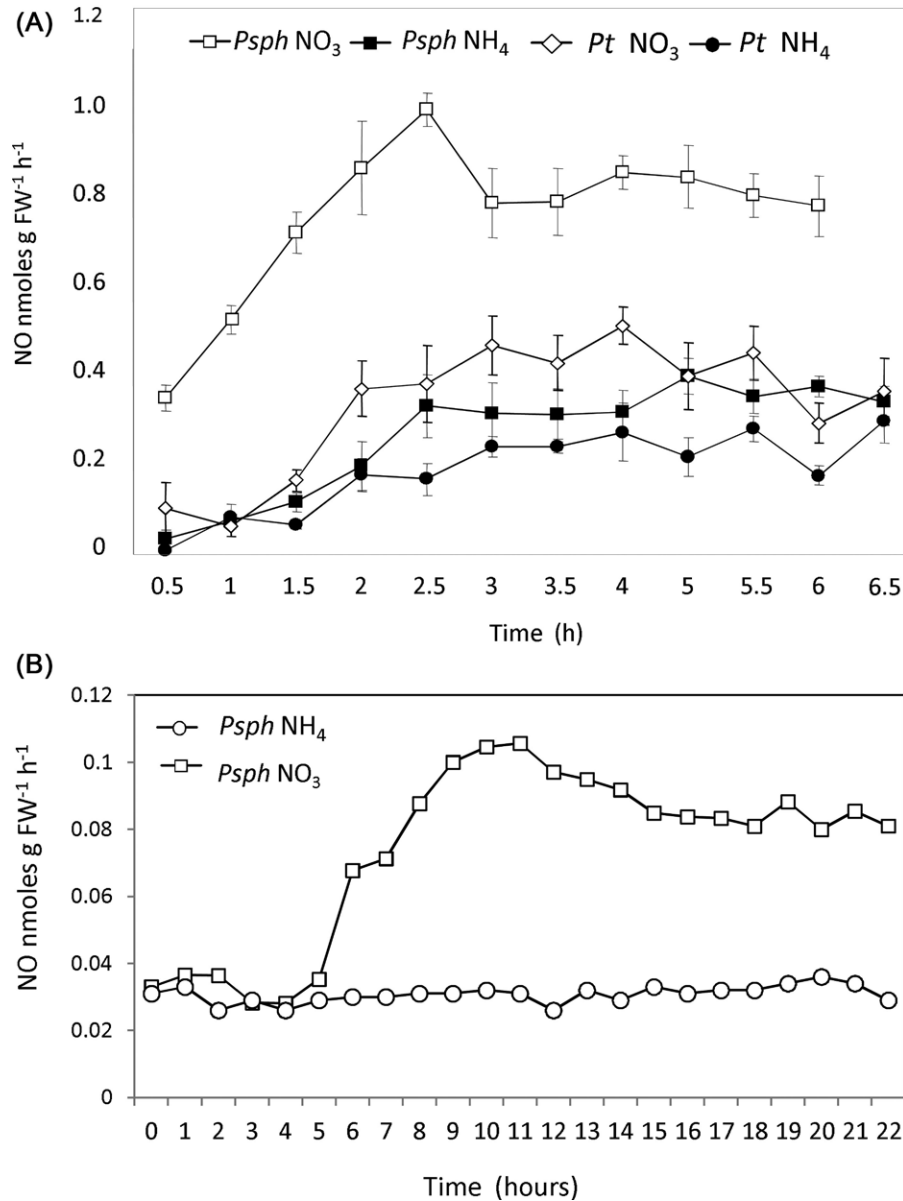


Fig. 2. NO production in *Psph*- and *Pt*-inoculated NO₃⁻-fed and NH₄⁺-fed tobacco. (A) NO production in NO₃⁻-fed and NH₄⁺-fed tobacco leaves challenged with avirulent *Psph* or virulent *Pt* measured using a QCL. No NO was detected in tobacco leaves infiltrated with 10mM MgCl₂ (data not shown). In these experiments, the tobacco plants were grown in low-nutrient compost supplemented with NH₄⁺ or NO₃⁻. (B) The results were partially replicated in hydroponically grown plants challenged with *Psph* where NO production was measured using chemiluminescence detection. Data from the QCL represent the results of three separate experiments. Data from chemiluminescence represent results from two independent experiments.

Nitrate nutrition enhances PR1 gene expression and SA accumulation

To assess other effects of N nutrition on the HR, we examined the expression of a range of *pathogenesis-related* (*PR*) genes that respond to different signals using qRT-PCR. Given our focus on the HR, all subsequent experimentation used the avirulent strain *Psph*. Transcript levels of individual genes were normalized to the transcripts level of EF-1a to allow relative quantification of gene expression. This indicated that only *PR1a* expression induction was significantly ($P < 0.05$) reduced at 24h p.i. with NH₄⁺ compared with NO₃⁻ feeding

(Fig. 3A). No clear differential expression between N treatments was observed at 4 and 8 h p.i. (data not shown). The effects of NO₃⁻ feeding appeared to dominate over those of NH₄⁺ feeding, as co-application reversed the effects of the latter. *PR1a* is a biomarker for SA-mediated resistance (Delaney et al., 2004), so we quantified SA accumulation at 4, 8, and 24 h p.i. with *Psph* (Fig. 3B). No elevation in total SA levels was observed compared with uninfected controls until 24 h p.i. At this time point, NO₃⁻-fed plants accumulated more SA than NH₄⁺-fed tobacco levels.

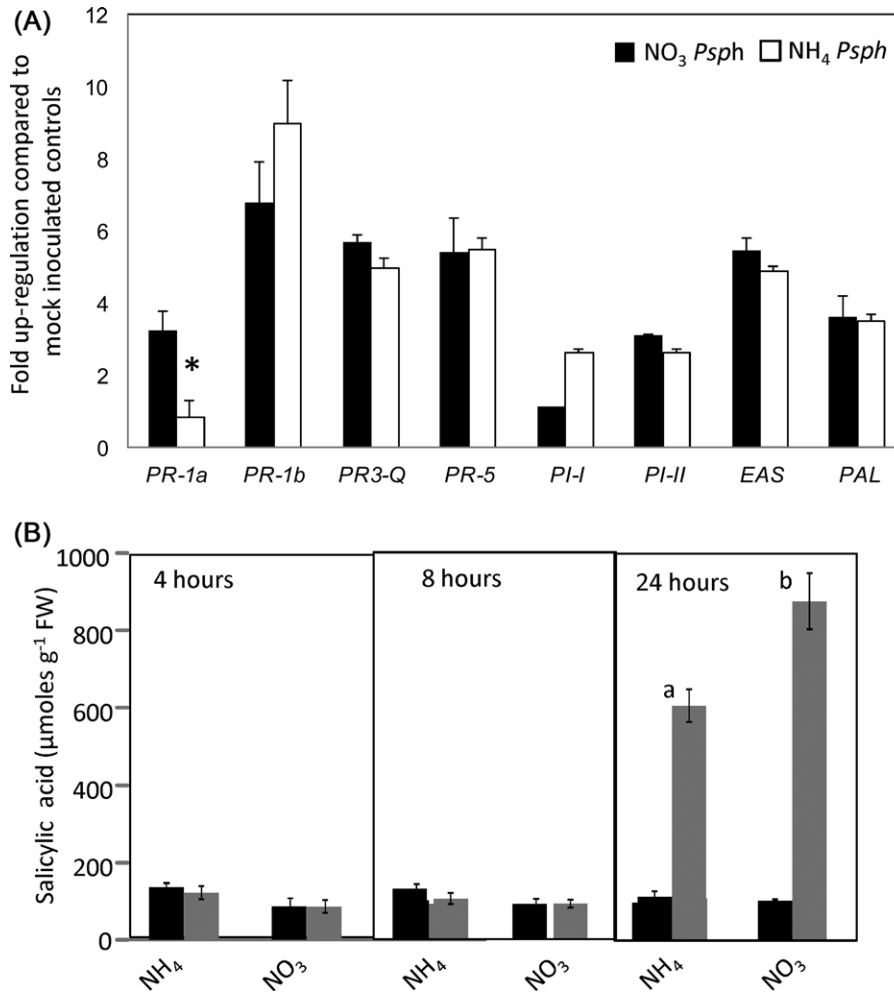


Fig. 3. Defence gene expression and SA accumulation in *Psph*-infected NO₃⁻-fed or NH₄⁺-fed tobacco leaves. (A) Fully expanded leaves of 4-week-old tobacco leaves were infiltrated with *Psph* and RNA was extracted from samples harvested at 24 h p.i. qRT-PCR was carried out as described in Material and methods with primers designed to detect transcripts of the following defence genes: *pathogenesis-related protein 1a* (*PR1a*) acidic form; *pathogenesis-related protein 1b* (*PR1b*) basic form; *pathogenesis-related protein 3 – Q* (*PR3-Q*, chitinase); *pathogenesis-related protein 5* (*PR-5*, thaumatin-like protein), *proteinase inhibitor I* (*PI-I*), *proteinase inhibitor II* (*PI-II*), *5-epi-aristolochene synthase* (*EAS*), and *phenylalanine ammonia lyase* (*PAL*) involved in phytoalexins biosynthesis. Transcripts were normalized to expression of the *EF-1a* housekeeping gene and results are expressed as fold increase or decrease compared with mock-inoculated controls. Results where significant differences ($P < 0.05$) were observed with different forms of N nutrition are indicated with an asterisk. (B) Free SA content of *Psph*-challenged (grey bars) and 10 mM MgCl₂-infiltrated (black bars) tobacco leaves at 4, 8, and 24 h p.i. in plants fed with NO₃⁻ or NH₄⁺. Data are given as mean µmoles g⁻¹ fresh weight (FW) ($n=4 \pm SD$). The results of *t*-tests showing significant differences ($P < 0.05$) compared with mock-inoculated controls are indicated with 'a'. Significant differences ($P < 0.05$) in NO₃⁻-fed compared with NH₄⁺-fed plants are indicated with 'b'.

Increased amino acid and sugar content in NH₄⁺-fed tobacco

To assess whether or not the pre-inoculation nutrient status of the plant could be a factor in the differential responses, a series of generalized biochemical assays were undertaken. Assessment of total amino acids indicated that these were significantly ($P < 0.001$) elevated in NH₄⁺-fed compared with NO₃⁻-fed tobacco plants (Fig. 4A). The response of sugar levels to NH₄⁺ and NO₃⁻ feeding in uninfected tobacco was also assessed both within the cell and in the apoplast. Both cytosolic and apoplastic sugar (sucrose, fructose, and glucose) contents were much higher in NH₄⁺-grown plants

(Fig. 4B, C). This suggested either that both sugar synthesis and sugar export are increased by NH₄⁺ nutrition, or possibly that sugar consumption is suppressed. Due to the very minute sample volume obtained, it was not technically feasible to measure apoplastic amino acid levels.

Metabolomic characterization of NO₃⁻ and NH₄⁺ effects following inoculation with *Psph*

Metabolic profiling approaches were followed to characterize further the effects of NO₃⁻ and NH₄⁺ nutrition of tobacco following challenge with *Psph*. Extracts of *Psph* and mock-inoculated (10 mM MgCl₂) samples were analysed

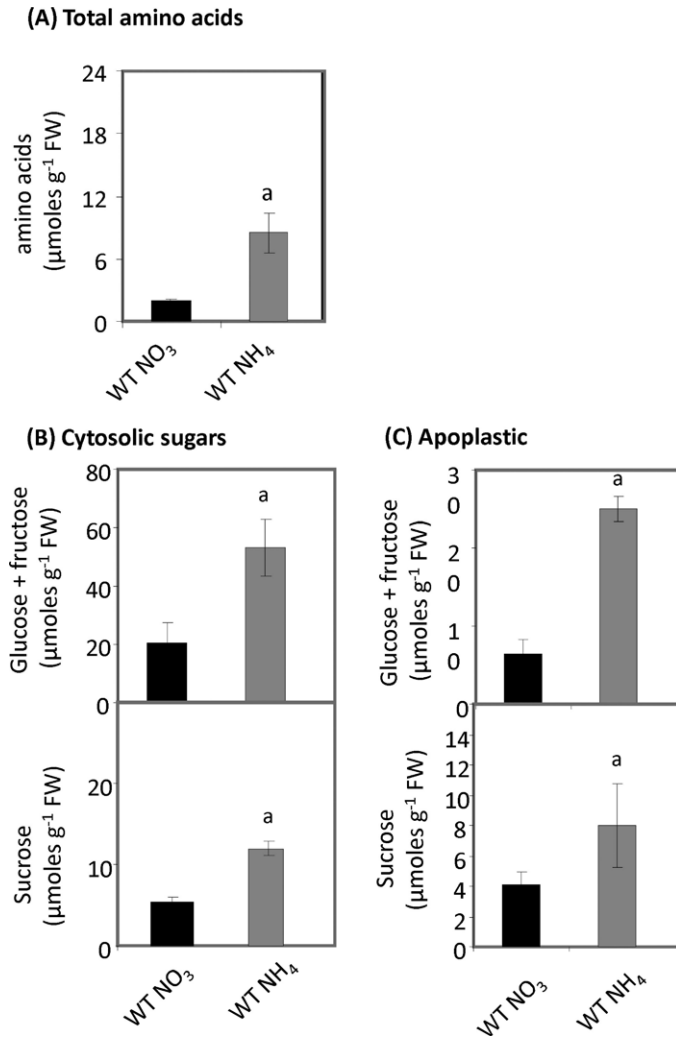


Fig. 4. Amino acid and hexose sugar accumulation in NO₃-fed and NH₄⁺-fed tobacco leaves. (A) Amino acid levels ($\mu\text{moles g}^{-1}$ FW) in tobacco leaves of wild-type plants fed NO₃ (black bars) or NH₄⁺ (grey bars). Data were obtained from eight leaves of eight independent plants. The plants were not inoculated with *PspH*. (B, C) Total hexose (glucose, fructose, and sucrose levels; $\mu\text{moles g}^{-1}$ FW) in the cytoplasm (B) or apoplasm (C) of tobacco leaves of wild-type plants fed NO₃ (black bars) or NH₄⁺ (grey bars). Data were obtained from eight leaves from eight different plants and are shown as means \pm SD. The isolation of apoplastic solutions is described in Materials and methods. The plants were not inoculated with *PspH*. Results showing a significant ($P < 0.05$) increase over NO₃-fed plants are indicated with 'a'.

by GC-MS, as described previously (Lisec *et al.*, 2006). The derived data were examined initially using non-supervised principal component analysis (PCA), and discrimination between NO₃⁻ and NH₄⁺, mock and infected material was observed only at 24h p.i. (Supplementary Fig. S2 at *JXB* online). To ease interpretation of these complicated data sets, they are also presented as a series of subanalyses separately examining GC-MS profiles from mock-inoculated samples (Fig. 5A), NO₃⁻-treated (Fig. 5B), and NH₄⁺-treated (Fig. 5C) plants. In mock-inoculated samples, NO₃⁻ and NH₄⁺

effects were relatively poorly differentiated except the 24h samples which partially separated along principal component 2 (PC2) (Fig. 5A). Based on the loading vectors for PC1 and PC2 (Supplementary Table S1 at *JXB* online), the most important metabolites contributing to this model appeared to be fumarate and malate, with subsidiary contributions by the amino acids glutamate, glutamine, and proline, as well as inositol and galactose (Fig. 5A). In Fig. 5B and C, PCA discriminated between *PspH* and mock-inoculated samples, allowing the loading vectors linked to metabolites making major contributions to the observed biological effects to be identified (Supplementary Table S1). Examining the effects of *PspH* challenge of NO₃⁻-fed tobacco suggested that, besides those metabolites indicated in Fig. 5A, changes in spermidine and putrescine were important sources of variation (Fig. 5B). With NH₄⁺ feeding, GABA and putrescine were additional sources of variation over baseline changes, as suggested from an analysis of the mock-inoculated controls (Fig. 3C). Based on the detected metabolites, these observations suggested that two pathways were prominent sources of differentiation between the NO₃⁻ and NH₄⁺ effects on the *PspH*-induced HR: respectively, the polyamine and GABA/TCA cycle metabolites.

The metabolites that form the glutamine–polyamine pathways were examined in isolation (Fig. 6). Challenge with *PspH* increased the concentrations of glutamine (Fig. 6A) and glutamate (Fig. 6B) but not ornithine (Fig. 6), whether plants were fed NO₃⁻ or NH₄⁺. Interestingly, citrulline, which is produced from ornithine, exhibited a feeding-specific effect (Fig. 6D). However, proline, which is produced from glutamate, exhibited no infection or nutrition-specific trend (Fig. 6E). Thus, although proline was prominent in the loading vectors that discriminated between the treatment groups (Fig. 5), it could not be readily related to a biological response. By contrast, an alternative pathway leading to putrescine (Fig. 6F) increased with infection following both NO₃⁻ and NH₄⁺ feeding. However, different N feeding appeared to encourage a differential processing of putrescine and linked metabolites. At 24h p.i., a pathway leading to GABA formation appeared to be particularly prominent in NH₄⁺-fed plants following infection (Fig. 6G), whilst an alternative pathway leading to spermidine accumulation appear to predominate with infected and NO₃⁻-fed plants (Fig. 6H).

The accumulation of GABA led us to examine the accumulation of metabolites that could be linked to the GABA shunt/TCA cycle (Fig. 7A). Succinate, malate, and fumarate (Fig. 7D–F) showed increased accumulation on infection with either NO₃⁻-fed or NH₄⁺-fed plants, but at 24h p.i., all also exhibited significantly greater accumulation in NH₄⁺ plants. These observations suggested increased TCA cycle activity in line with the energetic demands of plant defence. In addition, given the increased accumulation of glutamate and GABA (Fig. 7B, C), it is likely that the GABA shunt is a more marked feature of NH₄⁺-fed plants.

Galactose was prominent in the loading vectors that discriminated between the experimental treatments (Fig. 5). The data for this metabolite were plotted to indicate significantly greater accumulation in *PspH*-challenged NH₄⁺-fed tobacco

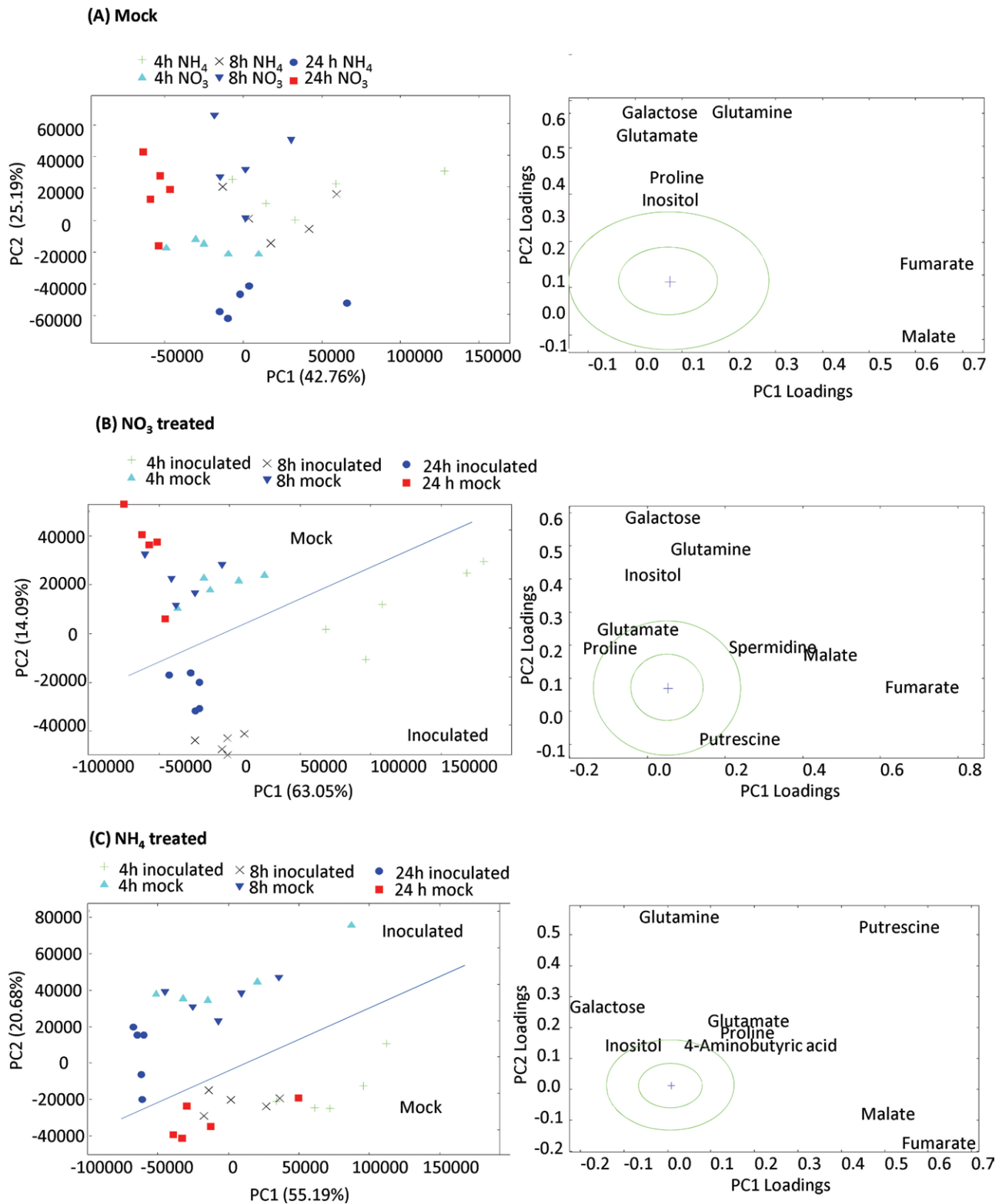


Fig. 5. Identifying metabolite changes occurring in NO₃⁻ or NH₄⁺ in tobacco leaves following inoculation with *PspH*. Results are shown for PCA of 150 metabolites detected by GC-MS in NO₃⁻-fed and NH₄⁺-fed tobacco leaves following infiltration with 10 mM MgCl₂ (mock inoculated) (A), and NO₃⁻-treated and *PspH* challenged plants (B) or NH₄⁺-treated and *PspH* challenged plants (C). In each case, samples were analysed at 4, 8, and 24 h following inoculation. In (B) and (C), clear separation between mock- and *PspH*-inoculated plants is delineated and labelled. In (A–C), the loading vectors (listed in [Supplementary Table S1](#)) used for the corresponding PC1 and PC2 are plotted. The '+' marks the zero point where loading vectors associated with metabolites make no contribution to the plot shown in (B), whilst the circles correspond to 1 and 2 SD from this zero point. Thus, the metabolites that are major sources of variation are shown.

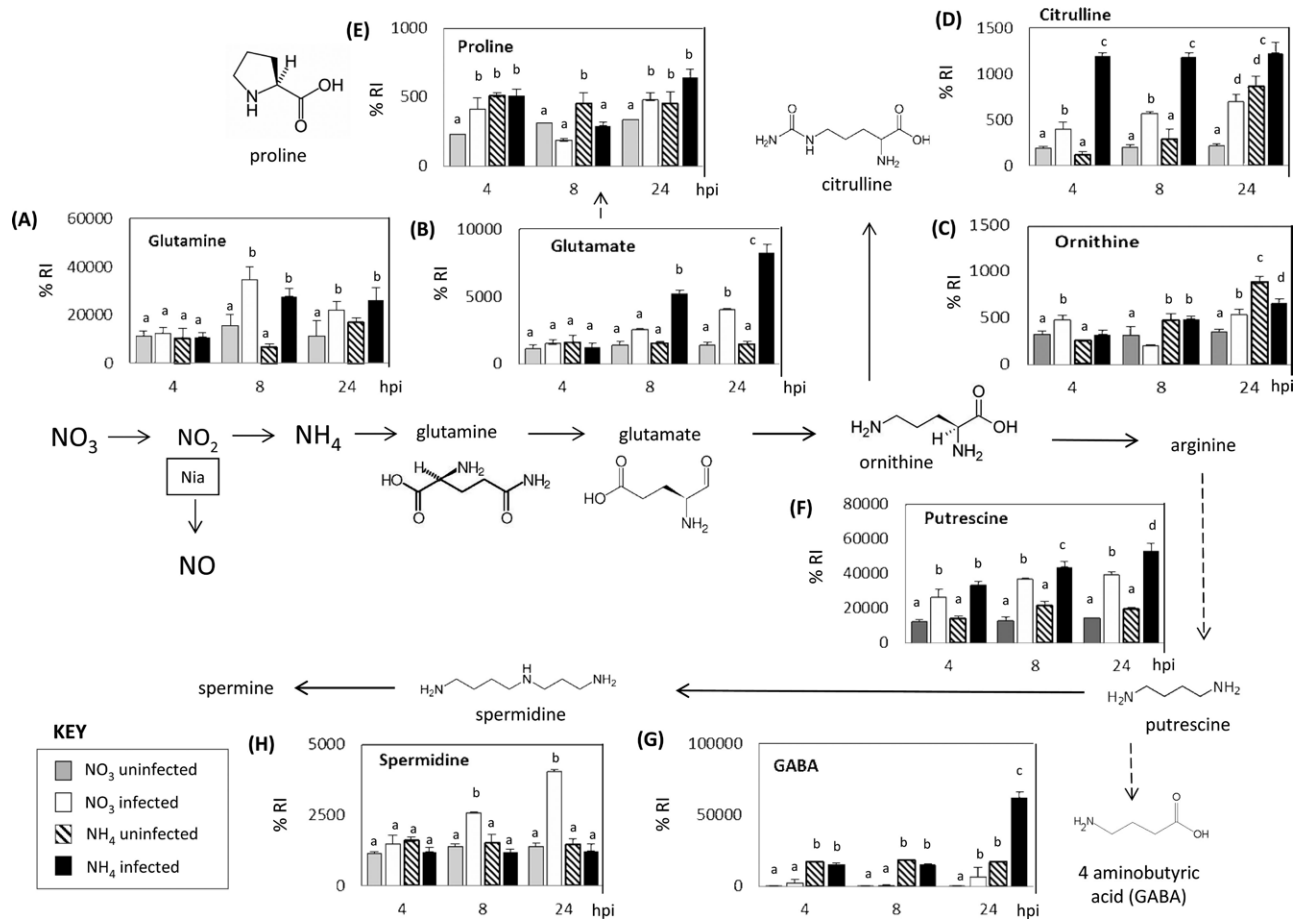


Fig. 6. N-assimilatory proline and putrescine pathways in the responses of tobacco to *PspH*. Results from individual metabolites are displayed around the assimilatory pathway of NO_3^- and NH_4^+ in plants linking through to proline, polyamine, and GABA. Note the position of NR encoded by the *nia* gene and its role in N assimilation and NO generation. The pathways were adapted from the Plant Metabolic network (<http://www.plantcyc.org/>). Broken arrows indicate multiple steps. Metabolites were detected by GC-MS in NO_3^- -fed and NH_4^+ -fed tobacco leaves following inoculation with *PspH* or mock inoculation with 10 mM MgCl_2 . Results are shown for glutamine (A), glutamate (B), ornithine (C), citrulline (D), proline (E), putrescine (F), GABA (G), and spermidine (H). Data are displayed as the percentage of relative intensity (% RI). Different letters denote groupings within which non-significant differences were observed but which were significantly different ($P < 0.05$) from all other groups.

compared with similarly inoculated NO_3^- -fed tobacco (Supplementary Fig. 3 at *JXB* online). Galactose accumulation in plants could occur as part of the biosynthesis of ascorbate (Laing et al., 2007) or the construction of cell-wall polymers (Seifert et al., 2002). In Supplementary Fig. S3, the data are displayed in terms of the role of galactose in contributing to glycolysis (Plaxton, 1996), as this could be part of the biogenetic changes occurring following *PspH* challenge. However, the accumulation patterns of other glycolysis-associated metabolites did not correlate with the treatment classes. Inositol also was also highlighted in the list of metabolites that discriminated between the experimental classes (Fig. 5). However, when considering the inositol data in isolation, they did not indicate a clear, biologically relevant trend (Supplementary Fig. S4A at *JXB* online). This was also the case with all other amino acids measured by GC-MS (Supplementary Fig. S4).

Discussion

A major driver for increased agricultural production in the 20th century has been the extensive use of N fertilizers (Tilman et al., 2002). The increased availability of N is a direct consequence of the Haber–Bosch process where nitrogen gas (N_2) is fixed to form NH_3 as the end product. NH_3 is used to derive N fertilizers such as anhydrous ammonium nitrate (NH_4NO_3) and urea [$\text{CO}(\text{NH}_2)_2$]. Within the soil ecosystem, the applied NH_4 is readily oxidized by microbial nitrification processes to form NO_3^- . NO_3^- is the main source of inorganic N for plants, but mainly due to the negative charge of clay, is easily leached out of soil to become a major water pollutant and a source of eutrophication (Peng and Zhu, 2006). NO_3^- removal is an expensive process so alternative strategies, including the use of nitrification inhibitors, have been followed (de Klein et al., 1996). Such measures illustrate how N fertilizer will continue to

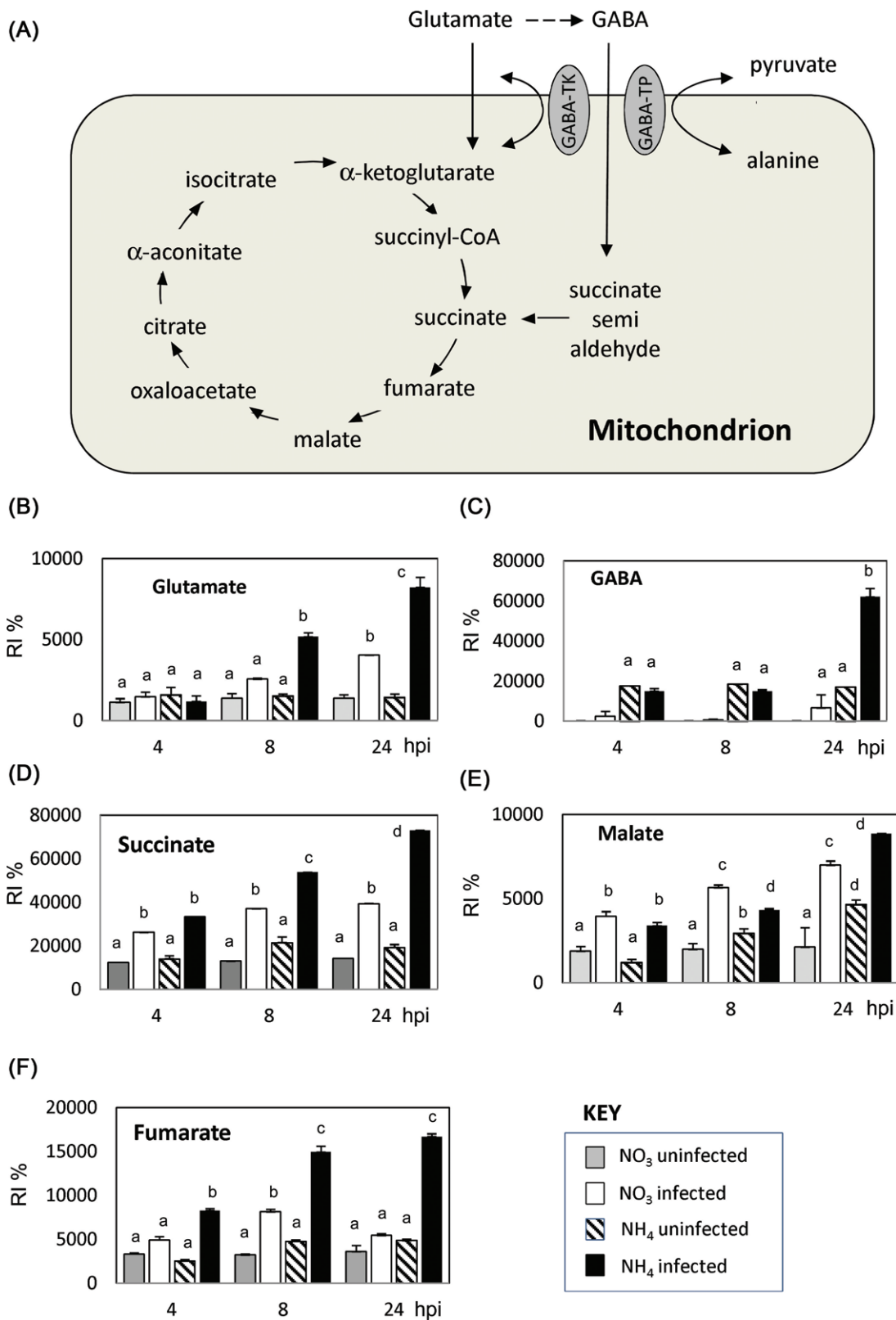


Fig. 7. Changes in the TCA cycle/GABA shunt in NO₃⁻-fed and NH₄⁺-fed tobacco leaves following inoculation with *Psph*. (A) Depiction of the TCA cycle linked to the GABA shunt. Metabolites were detected by GC-MS in NO₃⁻-fed and NH₄⁺-fed tobacco leaves following inoculation with *Psph* or mock inoculation with 10mM MgCl₂. Results are shown for glutamate (B), GABA (C), succinate (D), malate (E), and fumarate (F). Data are displayed as the percentage of relative intensity (% RI). Different letters denote groupings within which non-significant differences were observed but which were significantly different ($P < 0.05$) from all other groups.

feature in modern agriculture, so the wide-ranging effects of NO_3^- on plant physiology need to be fully assessed. The effects of different N forms have been investigated at the level of, for example, the response to elevated CO_2 (Geiger *et al.*, 1999) and indeed on disease development (Huber and Watson, 1974), but there has been much less work done with respect to the HR. New diseases are constantly emerging and although R gene-mediated, HR-linked defences are often ephemeral (Stuthman, 2002), they continue to be important components of crop breeding programmes. It is therefore vital to identify and characterize agricultural and horticultural practices that could compromise or increase these R gene-linked defence mechanisms. Thus, here we sought to characterize the effects of NO_3^- and NH_4^+ feeding of tobacco plants on a HR elicited by *PspH*.

NO⁻ and SA-mediated defence is augmented by NO⁻ nutrition

To assess the effects of variable N-form nutrition, we made use of hydroponically fed tobacco plants (Kaiser *et al.*, 2004, 2005). In our experimental approach, we did not observe any effects of NH_4^+ feeding on tobacco growth or biomass, as observed by Walch-Liu *et al.* (2000), which may reflect our use of cv. Gatersleben compared with cv. Samsun. The lack of any NH_4^+ toxicity was also suggested from the lack of significant treatment-specific effects on *EFL1* expression in our qRT-PCR analysis (data not shown).

Our initial assessments suggested that NO_3^- nutrition influenced cell death but that NH_4^+ feeding had a greater impact on mechanisms that suppressed bacterial growth during the HR (Fig. 1). When considering how NO_3^- could be contributing to cell death, one of the most likely routes is via NO production (Romero-Puertas *et al.*, 2004). Many sources of NO generation have been proposed, including the oxidation of L-arginine or polyamines by as yet poorly characterized enzymatic sources. However, one of the most well established is the NAD(P)H-linked reduction of NO_3^- by cytosolic NR (Rockel *et al.*, 2002). N assimilation by NH_4^+ rather than NO_3^- would therefore effectively short-circuit NO production if NR was a major source of NO during the *PspH*-elicited HR in tobacco. Our assessments of NO production from *Nia30* plants demonstrated that this was the major source of NO during the *PspH*-elicited HR of tobacco (Supplementary Fig. S1). Given this, it was telling that significantly ($P < 0.001$) more NO was generated in NO_3^- -fed as opposed to NH_4^+ -fed tobacco (Fig. 2A). This important observation indicated that some of the effects of reduced NO generation could be reproduced through simple nutritional effects and thus is of greater relevance to agricultural practice. Interestingly, citrulline accumulation was prominent in *PspH*-infected tobacco plants (Fig. 6D, which might be expected if an NO synthase (NOS)-like mechanism was contributing to NO production (NOS oxidizes arginine to produce NO and citrulline). However, this was considered to be unlikely, as citrulline accumulation was greatest in NH_4^+ -fed plants where NO production was reduced compared with NO_3^- -fed tobacco (Fig. 2).

NO also contributes to the initiation of SA biosynthesis (Durner and Klessig, 1999), and SA potentiates the oxidative

burst to augment cell death during the HR (Mur *et al.*, 2000). Thus, the reduction in SA accumulation at 24h p.i. in NH_4^+ -fed tobacco (Fig. 3B) is most likely linked to lower NO production (Fig. 2). It was also notable that, in our assessments of defence genes, expression in NH_4^+ effects seemed to be confined to the SA-regulated *PR1* gene. However, this need not indicate that reduced *PR1a* expression itself must be the cause of reduced resistance, as, although it is a well-established marker for plant defence (Hoof van Huijsduijnen *et al.*, 1985), its actual action is poorly defined (Alexander *et al.*, 1993; van Loon *et al.*, 2006). Other defence genes such as proteinase inhibitors were apparently not affected by N feeding. Fritz *et al.* (2006b) noted that expression of phenylalanine ammonia lyase (PAL), which plays a key role in phenylpropanoid production, was influenced by NO_3^- . Given the central role of PAL in plant defence (Pallas *et al.*, 1996) regulating the production of, for example, defence lignin, if NH_4^+ affects PAL expression, this could be a major source of compromised resistance. However, we did not observe any significant effect on PAL expression (Fig. 3A), suggesting that modulation of phenylpropanoid biosynthesis was not a source of loss of resistance following NH_4^+ treatment.

NH⁺ nutrition shifts the host responses to favour pathogenesis

In order to characterize further the N nutritional effects on defence, we chose to concentrate on metabolomic approaches with a focus on C:N primary metabolism. It could be predicted that the most obvious effect of differential N treatment would be wide-ranging changes in the concentrations of several amino acids. In fact, other than for a few examples (discussed below), most changes proved to be difficult to link with any biological effect (Supplementary Fig. S4). Within the context of NO_3^- -mediated resistance, metabolite profiling suggested the importance of polyamine production. Independent evidence also supports an important role for polyamines in defence (Walters, 2003). For example, elevation of spermine accumulation in transgenic lines increased resistance in tobacco against *Pt* and also the hemibiotrophic oomycete *Phytophthora parasitica* var. *nicotiana* (Moschou *et al.*, 2009), whilst increases in spermine in *Arabidopsis* boosted defence against *Pseudomonas viridiflava* (Gonzalez *et al.*, 2011). Mechanistically, polyamines could increase resistance by acting as substrates for a NO-generating complex (Yamasaki and Cohen, 2006), but are known to contribute to reactive oxygen species production and cell death (Cona *et al.*, 2006), as well as cell-wall reinforcement via conjugation to hydroxycinnamic acid (Walters, 2003). Whatever mechanisms are employed by polyamine, it is apparent that NO_3^- feeding alone is insufficient to trigger the shift to polyamine synthesis but requires additional elicitation by *PspH*.

Coupled to NO_3^- effects, we examined how NH_4^+ could compromise resistance and/or promote disease. *Nia30* mutants lacking NR have much lower levels of amino acids (Fritz *et al.*, 2006b), so we could have predicted that NH_4^+ feeding would reduce amino acid levels. However, instead we observed that there were increases in total amino acid levels with NH_4^+

feeding (Fig. 4). An alternative hypothesis could be related to the effects on carbon metabolism, as this is intimately related to N effects. Thus, for example, a suppression of carbon fixation by, for example, the generation of *RbcS* antisense plants reduces both carbohydrate concentrations and NO_3^- assimilation (Matt *et al.*, 2002). Indeed, sugar depletion can suppress *NIA* expression and NR activity (Matt *et al.*, 2002), whilst the application of sugar can reverse this effect (Koch, 1996), as well as inducing nitrate transporter genes (Lejay *et al.*, 1999). Correspondingly, glucose and sucrose concentrations are reduced in NO_3^- -depleted tobacco (Fritz *et al.*, 2006a). Given this, it is significant that, in NH_4^+ -fed plants, there were increases cellular and apoplastic hexose levels compared with NO_3^- (Fig. 4). This would be a direct advantage to apoplastically located bacterial pathogens (Rico and Preston, 2008). Sucrose was also noted to increase in *Arabidopsis* when challenged with *P. syringae* pv. *tomato* (Ward *et al.*, 2010), further suggesting that this is an important feature of disease development.

Given these observations, it is worth highlighting the similarity of some events during disease development and N mobilization during senescence (Masclaux-Daubresse *et al.*, 2006, 2007). Senescence is characterized by the mobilization of nitrogen, carbon, and other nutrients out of the leaf to other parts of the plant or to contribute to such reproductively important processes as grain filling (Buchanan-Wollaston, 1997). Prominent senescence-linked changes include the export of hexose sugars from the cell. Similarly, the mobilization of starch and sucrose export is a feature of many disease situations (Scharte *et al.*, 2005; Swarbrick *et al.*, 2006; Essmann *et al.*, 2008). Indeed, a causal link between sugar export and disease symptom development has been demonstrated (Kocal *et al.*, 2008). Therefore, it is possible that NH_4^+ feeding encourages disease development by promoting a leaf senescence programme. This effect may not be due directly to NH_4^+ but to a reduction in NO production during a HR. NO has been suggested to act as an anti-senescence signal (Mishina *et al.*, 2007), so a lowering of the NO concentration would actively promote senescence.

Our GC-MS analyses revealed a prominent accumulation of GABA following NH_4^+ feeding, representing a diversion of putrescine metabolism away from polyamine biosynthesis. Increases in GABA are a well-established feature of plant senescence (Masclaux *et al.*, 2000; Diaz *et al.*, 2005) and this could act as an enhancer of ethylene effects, represent a transient N storage compound or activation of the GABA shunt (Diaz *et al.*, 2005). Within the context of challenge of tobacco with *Psph*, GABA could serve directly as a nutrient source for pathogens (Kinnersley and Turano, 2000; Solomon and Oliver, 2001) but when coupled to increases in malate, fumarate, and especially succinate, it suggested that flux through the GABA shunt was enhanced (Fig. 7). The GABA shunt provides a metabolic route through which N input can feed directly into the TCA cycle and thus bioenergetically contribute to the mobilization of nutrients. As with polyamine metabolism, the shift to GABA was not prominent in solely NH_4^+ -fed plants but required challenge with *Psph*, which would suggest that a pathogen-elicited pathway was being altered. In the most comprehensive metabolomic investigation of plant disease,

Ward *et al.* (2010) noted only marginal increases in GABA in *Arabidopsis* following inoculation with *Pseudomonas syringae* pv. *tomato*. The lack of concordance between the two datasets could reflect differences between tobacco and *Arabidopsis*, or that, in our case, the NH_4^+ -modified HR only partially reflects a true disease scenario. Clearly, further work is required to characterize how changes in metabolite flux through putrescine with NO_3^- or NH_4^+ feeding are regulated, and these are currently underway in our laboratories.

Taken together, our observations demonstrate that N nutrition can either enhance or compromise *R* gene-mediated resistance. We have provided some mechanistic insight into these mechanisms by suggesting that NO_3^- is important for resistance, mostly via NO and SA generation, as well as polyamine biosynthesis. In contrast, feeding NH_4^+ can compromise resistance not only through reduced NO generation but also by encouraging metabolic reprogramming of HR defence towards sugar and GABA production. Crucially, if these data are extrapolated into an agricultural context, it seems likely that the form of N applied, as well as the levels, can influence susceptibility to pathogens in crop species.

Supplementary data

Supplementary are available at *JXB* online.

Supplementary Table S1. Loading vectors for PCA models shown in Fig. 5A–C, which analyse metabolite changes occurring in NO_3^- -fed or NH_4^+ -fed tobacco leaves following mock infection and inoculation with *Psph*.

Supplementary Fig. S1. Nitrate reductase-dependent effects on the HR elicited by *Psph* in tobacco.

Supplementary Fig. S2. Multivariate analyses of metabolite profiles of NO_3^- -fed and NH_4^+ -fed tobacco leaves following inoculation with *Psph*.

Supplementary Fig. S3. Galactose and glycolytic metabolite accumulation in NO_3^- -fed and NH_4^+ -fed tobacco leaves following inoculation with *Psph* or 10 mM MgCl_2 .

Supplementary Fig. S4. Amino acid accumulation in NO_3^- - and NH_4^+ -fed tobacco leaves following inoculation with *Psph* or 10 mM MgCl_2 .

Acknowledgements

We thank Lothar Willmitzer for critical reading of the manuscript and also for providing the GC-MS facilities, Eva Wirth for amino acid analysis, and Maria Lesch for technical assistance. We also thank the anonymous referees for making some important suggestions. This work was supported by DFG (SFB 567) to W.M.K. and K.J.G. and the Max Planck Society (K.J.G., Y.B., and S.S.).

References

- Alexander D, Goodman RM, Gutrella M, *et al.* 1993. Increased tolerance to two oomycete pathogens in transgenic tobacco expressing pathogenesis-related protein-1a. *Proceedings of the National Academy of Sciences U S A* **90**, 7327–7331.

- Arvidsson S, Kwasniewski M, Riano-Pachon DM, Mueller-Roeber B.** 2008. QuantPrime—a flexible tool for reliable high-throughput primer design for quantitative PCR. *BMC Bioinformatics* **9**, 465.
- Bauwe H, Hagemann M, Fernie AR.** 2010. Photorespiration: players, partners and origin. *Trends in Plant Science* **15**, 330–336.
- Bender CL, Alarcon-Chaidez F, Gross DC.** 1999. *Pseudomonas syringae* phytotoxins: mode of action, regulation, and biosynthesis by peptide and polyketide synthetases. *Microbiology and Molecular Biology Reviews* **63**, 266–292.
- Buchanan-Wollaston V.** 1997. The molecular biology of leaf senescence. *Journal of Experimental Botany* **48**, 181–199.
- Clarke SM, Mur LA, Wood JE, Scott IM.** 2004. Salicylic acid dependent signaling promotes basal thermotolerance but is not essential for acquired thermotolerance in *Arabidopsis thaliana*. *The Plant Journal* **38**, 432–447.
- Cona A, Rea G, Angelini R, Federico R, Tavladoraki P.** 2006. Functions of amine oxidases in plant development and defence. *Trends in Plant Science* **11**, 80–88.
- Cristescu SM, Persijn ST, te Lintel Hekkert S, Harren FJM.** 2008. Laser-based systems for trace gas detection in life sciences. *Applied Physics B—Lasers and Optics* **92**, 343–349.
- Cuadros-Inostroza A, Caldana C, Redestig H, Kusano M, Lisec J, Pena-Cortes H, Willmitzer L, Hannah MA.** 2009. TargetSearch—a Bioconductor package for the efficient preprocessing of GC-MS metabolite profiling data. *BMC Bioinformatics* **10**, 428.
- Dannel F, Pfeffer H, Marschner H.** 1995. Isolation of apoplasmic fluid from sunflower leaves and its use for studies on influence of nitrogen supply on apoplasmic pH. *Journal of Plant Physiology* **50**, 208–213.
- de Klein CAM, van Logtestijn RSP, van de Meer HG, Geurink JH.** 1996. Nitrogen losses due to denitrification from cattle slurry injected into grassland soil with and without a nitrification inhibitor. *Plant and Soil* **183**, 161–170.
- Delaney TP, Uknes S, Vernooij B, et al.** 2004. A central role of salicylic acid in plant disease resistance. *Science* **1266**, 1247–1250.
- Delledonne M, Lamb C, Xia YJ, Dixon RA.** 1998. Nitric oxide functions as a signal in plant disease resistance. *Nature* **394**, 585–588.
- Diaz C, Purdy S, Christ A, Morot-Gaudry JF, Wingler A, Masclaux-Daubresse C.** 2005. Characterization of markers to determine the extent and variability of leaf senescence in *Arabidopsis*. A metabolic profiling approach. *Plant Physiology* **138**, 898–908.
- Durner J, Klessig DF.** 1999. Nitric oxide as a signal in plants. *Current Opinion in Plant Biology* **2**, 369–374.
- Espunya MC, De Michele R, Gomez-Cadenas A, Martinez MC.** 2012. S-Nitrosoglutathione is a component of wound- and salicylic acid-induced systemic responses in *Arabidopsis thaliana*. *Journal of Experimental Botany* **63**, 3219–3227.
- Essmann J, Schmitz-Thom I, Schon H, Sonnewald S, Weis E, Scharte J.** 2008. RNA interference-mediated repression of cell wall invertase impairs defense in source leaves of tobacco. *Plant Physiology* **147**, 1288–1299.
- Fait A, Fromm H, Walter D, Galili G, Fernie AR.** 2008. Highway or byway: the metabolic role of the GABA shunt in plants. *Trends in Plant Science* **13**, 14–19.
- Fritz C, Mueller C, Matt P, Feil R, Stitt M.** 2006a. Impact of the C-N status on the amino acid profile in tobacco source leaves. *Plant, Cell & Environment* **29**, 2055–2076.
- Fritz C, Palacios-Rojas N, Feil R, Stitt M.** 2006b. Regulation of secondary metabolism by the carbon-nitrogen status in tobacco: nitrate inhibits large sectors of phenylpropanoid metabolism. *The Plant Journal* **46**, 533–548.
- Fromm H, Bouche N.** 2004. GABA in plants: just a metabolite? *Trends in Plant Science* **9**, 110–115.
- Geiger M, Haake V, Ludewig F, Sonnewald U, Stitt M.** 1999. The nitrate and ammonium nitrate supply have a major influence on the response of photosynthesis, carbon metabolism, nitrogen metabolism and growth to elevated carbon dioxide in tobacco. *Plant, Cell & Environment* **22**, 1177–1199.
- Gonzalez ME, Marco F, Minguet EG, Carrasco-Sorli P, Blázquez MA, Carbonell J, Ruiz OA, Pieckenstein FL.** 2011. Perturbation of spermine synthase gene expression and transcript profiling provide new insights on the role of the tetraamine spermine in *Arabidopsis* defense against *Pseudomonas viridiflava*. *Plant Physiology* **156**, 2266–2277.
- Green PA, Vorosmarty CJ, Meybeck M, Galloway JN, Peterson BJ, Boyer EW.** 2004. Pre-industrial and contemporary fluxes of nitrogen through rivers: a global assessment based on typology. *Biogeochemistry* **68**, 71–105.
- Gullino ML, Kuijpers LAM.** 1994. Social and political implications of managing plant-diseases with restricted fungicides in Europe. *Annual Review of Phytopathology* **32**, 559–579.
- Gupta KJ, Fernie AR, Kaiser WM, van Dongen JT.** 2011. On the origins of nitric oxide. *Trends in Plant Science* **16**, 160–168.
- Gupta KJ.** 2011. Protein S-nitrosylation in plants: photorespiratory metabolism and NO signaling. *Science Signaling* **154**, Jc1.
- Hajjar R, Hodgkin T.** 2007. The use of wild relatives in crop improvement: a survey of developments over the last 20 years. *Euphytica* **156**, 1–13.
- Huber DM, Watson RD.** 1974. Nitrogen form and plant disease. *Annual Review of Phytopathology* **12**, 139–165.
- Jarvis RM, Broadhurst D, Johnson H, O'Boyle NM, Goodacre R.** 2006. PYCHEM: a multivariate analysis package for python. *Bioinformatics* **22**, 2565–2566.
- Kaiser WM, Planchet E, Sonoda M.** 2004. NO emission by plants, and sources for NO. *Nitric Oxide—Biology and Chemistry* **11**, 37–37.
- Kaiser WM, Planchet E, Gupta KJ, Sonoda M.** 2005. Nitric oxide emission from tobacco leaves and cell suspensions: rate limiting factors and evidence for the involvement of mitochondrial electron transport. *The Plant Journal* **41**, 732–743.
- Khokon MAR, Okuma E, Hossain MA, Munemasa S, Uraji M, Nakamura Y, Mori IC, Murata Y (2011).** Involvement of extracellular oxidative burst in salicylic acid-induced stomatal closure in *Arabidopsis*. *Plant Cell & Environment* **34**, 434–443.
- Kinnersley AM, Turano FJ.** 2000. Gamma aminobutyric acid (GABA) and plant responses to stress. *Critical Reviews in Plant Sciences* **19**, 479–509.

- Klessig DF, Durner J, Noad R, et al.** 2000. Nitric oxide and salicylic acid signaling in plant defense. *Proceedings of the National Academy of Sciences U S A* **97**, 8849–8855.
- Kocal N, Sonnewald U, Sonnewald S.** 2008. Cell wall-bound invertase limits sucrose export and is involved in symptom development and inhibition of photosynthesis during compatible interaction between tomato and *Xanthomonas campestris* pv *vesicatoria*. *Plant Physiology* **148**, 1523–1536.
- Koch KE.** 1996. Carbohydrate-modulated gene expression in plants. *Annual Review of Plant Physiology and Plant Molecular Biology* **47**, 509–540.
- Kopka J, Schauer N, Krueger S, et al.** 2005. GMD@CSB.DB: the Golm Metabolome Database. *Bioinformatics* **21**, 1635–1638.
- Laing WA, Wright MA, Cooney J, Bulley SM.** 2007. The missing step of the L-galactose pathway of ascorbate biosynthesis in plants, an L-galactose guanylyltransferase, increases leaf ascorbate content. *Proceedings of the National Academy of Science U S A* **104**, 9534–9539.
- Lejay L, Tillard P, Lepetit M, Olive F, Filleur S, Daniel-Vedele F, Gojon A.** 1999. Molecular and functional regulation of two NO₃⁻ uptake systems by N- and C-status of *Arabidopsis* plants. *The Plant Journal* **18**, 509–519.
- Libault M, Wan JR, Czechowski T, Udvardi M, Stacey G.** (2007) Identification of 118 *Arabidopsis* transcription factor and 30 ubiquitin-ligase genes responding to chitin, a plant-defense elicitor. *Molecular Plant-Microbe Interactions* **20**, 900–911.
- Lisec J, Schauer N, Kopka J, Willmitzer L, Fernie AR.** 2006. Gas chromatography mass spectrometry-based metabolite profiling in plants. *Nature Protocols* **1**, 387–396.
- Mahmood T, Voitke M, Gimmler H, Kaiser WM.** 2002. Sugar exudation by roots of *kallar grass* [*Leptochloa fusca* (L.) Kunth] is strongly affected by the nitrogen source. *Planta* **214**, 887–894.
- Masclaux C, Valadier MH, Brugiere N, Morot-Gaudry JF, Hirel B.** 2000. Characterization of the sink/source transition in tobacco (*Nicotiana tabacum* L.) shoots in relation to nitrogen management and leaf senescence. *Planta* **211**, 510–518.
- Masclaux-Daubresse C, Purdy S, Lemaitre T, Pourtau N, Taconnat L, Renou JP, Wingler A.** 2007. Genetic variation suggests interaction between cold acclimation and metabolic regulation of leaf senescence. *Plant Physiology* **143**, 434–446.
- Masclaux-Daubresse C, Reisdorf-Cren M, Pageau K, Lelandais M, Grandjean O, Kronenberger J, Valadier MH, Feraud M, Jouglet T, Suzuki A.** 2006. Glutamine synthetase–glutamate synthase pathway and glutamate dehydrogenase play distinct roles in the sink–source nitrogen cycle in tobacco. *Plant Physiology* **140**, 444–456.
- Matt P, Krapp A, Haake V, Mock HP, Stitt M.** 2002. Decreased Rubisco activity leads to dramatic changes of nitrate metabolism, amino acid metabolism and the levels of phenylpropanoids and nicotine in tobacco antisense RBCS transformants. *The Plant Journal* **30**, 663–677.
- Mishina TE, Lamb C, Zeier J.** 2007. Expression of a nitric oxide degrading enzyme induces a senescence programme in *Arabidopsis*. *Plant Cell & Environment* **30**, 39–52.
- Molodo LV, Augusto O, Almeida IMG, Magalhaes JR, Salgado I.** 2005. Nitrite as the major source of nitric oxide production by *Arabidopsis thaliana* in responses to *Pseudomonas syringae*. *FEBS Letters* **579**, 3814–3820.
- Moschou PN, Sarris PF, Skandalis N, Andriopoulou AH, Paschalidis KA, Panopoulos NJ, Roubelakis-Angelakis KA.** 2009. Engineered polyamine catabolism preinduces tolerance of tobacco to bacteria and oomycetes. *Plant Physiology* **149**, 1970–1981.
- Mur LA, Bi YM, Darby RM, Firek S, Draper J.** 1997. Compromising early salicylic acid accumulation delays the hypersensitive response and increases viral dispersal during lesion establishment in TMV-infected tobacco. *The Plant Journal* **12**, 1113–1126.
- Mur LA, Brown IR, Darby RM, Bestwick CS, Bi YM, Mansfield JW, Draper J.** 2000. A loss of resistance to avirulent bacterial pathogens in tobacco is associated with the attenuation of a salicylic acid-potentiated oxidative burst. *The Plant Journal* **23**, 609–621.
- Mur LA, Mandon J, Cristescu SM, Harren FJ, Prats E.** 2011. Methods of nitric oxide detection in plants: a commentary. *Plant Science* **181**, 509–519.
- Mur LAJ, Kenton P, Lloyd AJ, Ougham H, Prats E.** 2008. The hypersensitive response; the centenary is upon us but how much do we know? *Journal of Experimental Botany* **59**, 501–520.
- Pageau K, Reisdorf-Cren M, Morot-Gaudry JF, Masclaux-Daubresse C.** 2006. The two senescence-related markers GS1 (cytosolic glutamine synthetase) and GDH (glutamate dehydrogenase), involved in nitrogen mobilization, are differentially regulated during pathogen attack and by stress hormones and reactive oxygen species in *Nicotiana tabacum* L. leaves. *Journal of Experimental Botany* **57**, 547–557.
- Pallas JA, Paiva NL, Lamb C, Dixon RA.** 1996. Tobacco plants epigenetically suppressed in phenylalanine ammonia-lyase expression do not develop systemic acquired resistance in response to infection by tobacco mosaic virus. *The Plant Journal* **10**, 281–293.
- Peng YZ, Zhu GB** 2006. Biological nitrogen removal with nitrification and denitrification via nitrite pathway. *Applied Microbiology and Biotechnology* **73**, 15–26.
- Planchet E, Sonoda M, Gupta KJ, Kaiser WM.** 2005. Nitric oxide emission from tobacco leaves and cell suspensions: rate limiting factors and evidence for the involvement of mitochondrial electron transport. *The Plant Journal* **41**, 732–743.
- Plaxton WC.** 1996. The organization and regulation of plant glycolysis. *Annual Review of Plant Physiology and Plant Molecular Biology* **47**, 185–214.
- Pontier D, Gan SS, Amasino RM, Roby D, Lam E.** 1999. Markers for hypersensitive response and senescence show distinct patterns of expression. *Plant Molecular Biology* **39**, 1243–1255.
- Quirino BF, Normanly J, Amasino RM.** 1999. Diverse range of gene activity during *Arabidopsis thaliana* leaf senescence includes pathogen-independent induction of defense-related genes. *Plant Molecular Biology* **40**, 267–278.
- Rico A, Preston GM.** 2008. *Pseudomonas syringae* pv. *tomato* DC3000 uses constitutive and apoplast-induced nutrient assimilation pathways to catabolize nutrients that are abundant in the tomato apoplast. *Molecular Plant-Microbe Interactions* **21**, 269–282.

- Rockel P, Strube F, Rockel A, Wildt J, Kaiser WM.** 2002. Regulation of nitric oxide (NO) production by plant nitrate reductase *in vivo* and *in vitro*. *Journal of Experimental Botany* **53**, 103–110.
- Romero-Puertas MC, Perazzolli M, Zago ED, Delledonne M.** 2004. Nitric oxide signalling functions in plant–pathogen interactions. *Cellular Microbiology* **6**, 795–803.
- Rommens CM, Kishore GM.** 2000. Exploiting the full potential of disease-resistance genes for agricultural use. *Current Opinion in Biotechnology* **11**, 120–125.
- Scharte J, Schon H, Weis E.** 2005. Photosynthesis and carbohydrate metabolism in tobacco leaves during an incompatible interaction with *Phytophthora nicotianae*. *Plant Cell & Environment* **28**, 1421–1435.
- Schlesinger WH.** 2009. On the fate of anthropogenic nitrogen. *Proceedings of the National Academy of Sciences U S A* **106**, 203–208.
- Scott IM, Clarke SM, Wood JE, Mur LA.** 2004. Salicylate accumulation inhibits growth at chilling temperature in *Arabidopsis*. *Plant Physiology* **135**, 1040–1049.
- Seifert GJ, Barber C, Wells B, Dolan L, Roberts K.** 2002. Galactose biosynthesis in *Arabidopsis*: genetic evidence for substrate channeling from UDP-D-galactose into cell wall polymers. *Current Biology* **12**, 1840–1845.
- Snoeijs SS, Perez-Garcia A, Joosten MHAJ Pierre JGM, De Wit.** 2000. The effect of nitrogen on disease development and gene expression in bacterial and fungal plant pathogens. *European Journal of Plant Pathology* **106**, 493–506.
- Solomon PS, Oliver RP.** 2001. The nitrogen content of the tomato leaf apoplast increases during infection by *Cladosporium fulvum*. *Planta* **213**, 241–249.
- Steinfath M, Groth D, Lisek J, Selbig J.** 2008. Metabolite profile analysis: from raw data to regression and classification. *Physiologia Plantarum* **132**, 150–161.
- Stuthman DD.** 2002. Contribution of durable disease resistance to sustainable agriculture. *Euphytica* **124**, 253–258.
- Sweetlove LJ, Beard KFM, Nunes-Nesi A, Fernie AR, Ratcliffe RG.** 2010. Not just a circle: flux modes in the plant TCA cycle. *Trends in Plant Science* **15**, 462–470.
- Sun LR, Hao FS, Lu BS, Ma LY.** 2010. AtNOA1 modulates nitric oxide accumulation and stomatal closure induced by salicylic acid in *Arabidopsis*. *Plant Signaling & Behaviour* **5**, 1022–1024.
- Swarbrick PJ, Schulze-Lefert P, Scholes JD.** 2006. Metabolic consequences of susceptibility and resistance (race-specific and broad-spectrum) in barley leaves challenged with powdery mildew. *Plant Cell & Environment* **29**, 1061–1076.
- Tadege M, Bucher M, Stahl W, Suter M, Dupuis I, Kuhlemeier C.** 1998. Activation of plant defense responses and sugar efflux by expression of pyruvate decarboxylase in potato leaves. *The Plant Journal* **16**, 661–671.
- Tavernier V, Cadiou S, Pageau K, Lauge R, Reisdorf-Cren M, Langin T, Masclaux-Daubresse C.** 2007. The plant nitrogen mobilization promoted by *Colletotrichum lindemuthianum* in *Phaseolus* leaves depends on fungus pathogenicity. *Journal of Experimental Botany* **58**, 3351–3360.
- Thibaud MC, Gineste S, Nussaume L, Robaglia C.** 2004. Sucrose increases pathogenesis-related PR-2 expression in *Arabidopsis thaliana* through an SA-dependent but NPR1-independent signalling pathway. *Plant Physiology and Biochemistry* **42**, 81–88.
- Tilman D, Cassman KG, Matson PA, Naylor R, Polasky S.** 2002. Agricultural sustainability and intensive production practices. *Nature* **418**, 671–677.
- Tilman D.** 1999. Global environmental impacts of agricultural expansion: the need for sustainable and efficient practices. *Proceedings of the National Academy of Sciences U S A* **96**, 5995–6000.
- Hooft van Huijsduijnen RAM, Cornelissen BJC, Vanloon LC, Vanboom JH, Tromp M, Bol JF.** 1985. Virus-induced synthesis of messenger-RNAs for precursors of pathogenesis-related proteins in tobacco. *EMBO Journal* **4**, 2167–2171.
- van Loon LC, Rep M, Pieterse CMJ.** 2006. Significance of inducible defense-related proteins in infected plants. *Annual Review of Phytopathology* **44**, 135–162.
- Walch-Liu P, Neumann G, Bangerth F, Engels C.** 2000. Rapid effects of nitrogen form on leaf morphogenesis in tobacco. *Journal of Experimental Botany* **51**, 227–237.
- Walters DR.** 2003. Polyamines and plant disease. *Phytochemistry* **64**, 97–107.
- Ward JL, Forcat S, Beckmann M, et al.** 2010. The metabolic transition during disease following infection of *Arabidopsis thaliana* by *Pseudomonas syringae* pv. *tomato*. *The Plant Journal* **63**, 443–457.
- Yamasaki H, Cohen MF.** 2006. NO signal at the crossroads: polyamine-induced nitric oxide synthesis in plants? *Trends in Plant Science* **11**, 522–524.
- Zeier J, Delledonne M, Mishina T, Severi E, Sonoda M, Lamb C.** 2004. Genetic elucidation of nitric oxide signaling in incompatible plant-pathogen interactions. *Plant Physiology* **136**, 2875–2886.